Estimation of chlorophyll content in maize canopy using wavelet denoising and SVR method

Haojie Liu[1], Minzan Li[1,2], Junyi Zhang[2], Dehua Gao[1], Hong Sun[1*], Liwei Yang[1]

(1. *Key Laboratory of Modern Precision Agriculture System Integration Research, Ministry of Education, China Agricultural University, Beijing 100083, China*;

2. *Key Laboratory of Agricultural information acquisition technology, Ministry of Agriculture, China Agricultural University, Beijing 100083, China*)

Abstract: In order to estimate the chlorophyll content of maize plant non-destructively and rapidly, the research was conducted on maize at the heading stage using spectroscopy technology. The spectral reflectance of maize canopy was measured and processed following wavelet denoising and multivariate scatter correction (MSC) to reduce the noise influence. Firstly, the signal to noise ratio (SNR) and curve smoothness (CS) were used to evaluate the denoising effect of different wavelet functions and decomposition levels. As a result, the Sym6 wavelet basis function and the 5th level decomposition were determined to denoise the original signal. The MSC method was used to eliminate the scattering effect after denoising. Then three spectral ranges were extracted by interval partial least squares (IPLS) including the 525-549 nm, 675-749 nm and 850-874 nm. Finally, the chlorophyll content estimation model was developed by using support vector regression (SVR) method. The calibration R_c^2 of the SVR model was 0.831, the *RMSEC* was 1.3852 mg/L; the validation R_v^2 was 0.809, the RMSEP was 0.8664 mg/L. The results show that the SNR and CS indicators can be used to select the parameters for wavelet denoising and model can be used to estimate the chlorophyll content of maize canopy in the field.

Keywords: maize canopy, spectral reflectance, wavelet denoising, SVR model, chlorophyll content

DOI: 10.25165/j.ijabe.20181106.3072

Citation: Liu H J, Li M Z, Zhang J Y, Gao D H, Sun H, Yang L W. Estimation of chlorophyll content in maize canopy using wavelet denoising and SVR method. Int J Agric & Biol Eng, 2018; 11(6): 132–137.

1 Introduction

Chlorophyll content of crop is an important indicator to estimate crop growth status, and is one of bases for field fertilizer management. According to the spectral absorption properties of chlorophyll, spectral analysis technique is widely used as a fast and non-destructive method for crop chlorophyll content detection[1-4].

To estimate the chlorophyll content of maize, Ciganda et al.[5] constructed red edge chlorophyll index with red edge (720-730 nm) and near infrared (770-800 nm) spectral reflectance. Chen et al.[6] proposed a new spectral indicator named Double-peak Canopy Nitrogen Index (DCNI) which was used for maize nitrogen detection. Schlemmer et al.[7] reported that chlorophyll content can be accurately retrieved using green and red-edge chlorophyll indices using near infrared (780-800 nm) and either green (540-560 nm) or red-edge (730-750 nm) spectral bands at the canopy level. Rossini et al.[8] estimated temporal chlorophyll using a suite of vegetation indices and found a high correlation of over 0.8 between leaf chlorophyll content and narrowband spectral indices.

However, in the field application, the spectral reflectance of crop canopy is measured by the spectrometer. It is a combination signal from leaves, soil background and around environment, and influenced by the random noise. Thus, it is necessary to denoise the spectral reflectance data and select the sensitive wavebands to help improve the performance of estimation model in the field[9,10].

For data denoising, it is generally processed in the spatial-domain and the time-frequency domain. In the spatial domain, it is used to remove some unwanted components or features from a signal such as moving average method, Savitzky-Golay (SG) convolution smoothing method and derivative algorithm. The results of moving average method and SG method are limited by the size of smoothing window which may cause signal distortion[11]. Although the derivative operation is considered as an effective method to eliminate interference of background and improve resolution, it may reduce signal-to-noise ratio (SNR) of spectral reflectance by involving new noise[12].

Wavelet analysis is a kind of time-frequency local analysis method with the area of wavelet window fixed and window shape varying[13]. Wavelet transform not only has the characteristics of multi-resolution analysis, but also has the ability to represent the local characteristics of the signal in time and frequency domain, which can help to effectively remove noise. The effect of wavelet denoising depends on suitable basis functions and decomposition layer. Li et al.[14] established the tomato vitamin C content prediction model based on the wavelet denoising by the db6 wavelet and 5th layer decomposition. Likewise, Liang et al.[15] published that the Haar wavelet and 5th layer decomposition could help to reduce the noise influence of the spectral reflectance of wheat canopy. As mentioned above, choosing suitable wavelet

Received date: 2017-06-25 **Accepted date:** 2018-05-18

Biographies: Haojie Liu, PhD candidate, research interests: agricultural informatization, Email: hjliu267@163.com; **Minzan Li,** PhD, Professor, research interests: precision agriculture, Email:limz@cau.edu.cn; **Junyi Zhang**, PhD candidate, research interests: agricultural informatization, Email: junyizh@cau.edu.cn; **Dehua Gao**, PhD candidate, research interests: agricultural engineering, Email: 751723071@qq.com; **Liwei Yang**, PhD, Associate Professor, research interests: agricultural engineering, Email: yangliwei@cau.edu.cn.

*__Corresponding author: Hong Sun,__ PhD, Associate Professor, research interest: agricultural informatization. China Agricultural University, Beijing 100083, China. Tel: +86-10-62737924, Email: sunhong@cau.edu.cn.

parameters is important for spectrum denoising and chlorophyll detection modelling in the field.

In this research, to detect the chlorophyll content rapidly and non-destructively, the spectral reflectance of maize canopy was measured. To eliminate the noise influence, the wavelet parameters were discussed in detail. After the sensitive wavelengths selection, a chlorophyll content estimation model was established.

2 Materials and methods

2.1 Field experiment

The field experiment was conducted at the Shangzhuang Experimental Station of China Agricultural University (CAU) in Beijing on May 13, 2016. It was a sunny day and suitable for spectral reflectance measurement. The field area was about 100 m×30 m and divided into 80 sample plots. The maize cultivar was Nongda98. The phenological phase was heading stage with the height of 60-70 cm.

The canopy spectral reflectance was measured by a handheld spectrometer (ASD, FieldSpecHH) in the range of 325 nm to 1075 nm within 1 nm increments. The view angle was 25 ° and the measurement height was about 50 cm above the canopy. The spectral reflectance data were taken three times and the average values were calculated in each plot.

After spectral reflectance measurement, canopy leaves were cut and packed into sealed bags, and then the chlorophyll content were detected in the laboratory.

2.2 Chlorophyll content measurement

The chlorophyll content was measured by an ultraviolet spectrophotometer (UV752). Firstly, the surface of winter wheat leaves was cleared and the main stems were removed. Secondly, the leaves were cut and mixed evenly. 0.4 g leaves were soaked into 25 mL mixed liquor of 99% acetone and absolute ethanol with the proportion of 2:1 for 24 hours. In the process of soaking, the mixed liquor was shaked every 8 hours to help the chlorophyll extraction. The absorbance data in 645 nm and 663 nm were determined by spectrophotometer. The chlorophyll content of leaves was calculated according to the Equations (1) and (2):

$$C_a = 12.72A_{663} - 2.59A_{645} \quad (1)$$

$$C_b = 22.88A_{645} - 4.67A_{663} \quad (2)$$

where, A_{645} and A_{663} were the absorbance of 645 nm and 663 nm; C_a and C_b were chlorophyll *a* and chlorophyll *b* content (mg/L) respectively. The total amount of chlorophyll content C_t equaled to C_a plus C_b.

2.3 Data processing method

The data processing followed the steps of spectrum denoising, sample set division, sensitive wavebands selection and estimation model establishing. Firstly, the field spectral data was processed by wavelet noise reduction and multivariate scatter correction (MSC). Secondly, the sample set division was conducted by sample set partitioning based on joint x-y distance (SPXY) and sensitive wavebands were selected by interval partial least squares (IPLS). Finally, a support vector regression (SVR) model was established for chlorophyll content estimation.

2.3.1 Wavelet denoising

Wavelet theory is applicable to several subjects. All wavelet transforms may be considered as forms of time-frequency representation for continuous-time (analog) signals. The essence of wavelet denoising is that the signal corresponds to a series of coefficients after the wavelet transform. Small coefficients correspond to noises and large coefficients correspond to actual signal. And the wavelet coefficients which are greater than the threshold value should be retained and the wavelet coefficients which are less than the threshold value can be set to zero. Thus the noise can be eliminated by reconstructing the signal with the processed wavelet coefficients. The flow of wavelet denoising is shown in Figure 1.

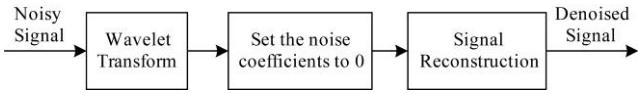

Figure 1 Flow chart of wavelet denoising

The wavelet toolbox was used and it could be conducted by the function: [xd, cxd, lxd]=wden（x, tptr, sorh, scal, n, ‘wname’）, in which x was the input signal. The ‘tptr’ specified the threshold selection rule. There are four options for ‘tptr’, specified as ‘rigrsure’, ‘sqtwolog’, ‘heursure’ and ‘minimaxi’. And the “heursure” rule was applied because of its robustness to small SNR signal. The ‘sorh’ parameter was specified as soft thresholding which was wavelet shrinkage. The ‘scal’ parameter was specified as ‘sln’ under the assumption of white noise. The ‘n’ parameter and ‘wname’ parameter defined the decomposition level and wavelet function respectively. The two factors had great influence on wavelet denoising effect. They were determined under the evaluation of the following SNR and curve smoothness (CS) indicators.

2.3.2 Evaluation of wavelet denoising effect

This study quantitatively evaluated the wavelet denoising effect by different wavelet basis functions and different decomposition layers. The evaluation was conducted by using the SNR indicator which is calculated according to Equation (3), and the CS indicator which is calculated according to Equation (4). The wavelet parameter was compared and selected by estimation of higher SNR and lower CS.

$$SNR = \frac{1}{N}\sum_{j=1}^{N} 10 \times \log_{10}\left(\sum_{i=1}^{L} \frac{x'^{\,2}_{ij}}{(x'_{ij} - x_{ij})^2}\right) \quad (3)$$

$$CS = \left\{\sum_{i=1}^{L}[x'_{i+1,j} - x'_{i,j}]^2\right\} / \left\{\sum_{i=1}^{L}[x_{i+1,j} - x_{i,j}]^2\right\} \quad (4)$$

where, x_{ij} is the original spectral reflectance of sample *j* at wavelength of *i* nm; x'_{ij} is the denoised spectral reflectance of the sample at waveband of *i* nm; *N* represents the number of samples, and *L* is the number of waveband per sample.

2.3.3 MSC

The MSC method[16,17] is a common method for eliminating baseline translation and shift caused by the overlap of leaves and soil background at the present stage. The method, conducted following Equations (5) and (6), could effectively eliminate scattering effects and enhance the relationship between spectral information and chlorophyll content.

$$X_i = a_i + b_i \overline{X_i} \quad (5)$$

$$X_{i\_msc} = (X_i - a_i) / b_i \quad (6)$$

where, X_i is the reflectance spectrum of the *i*-th sample; $\overline{X_i}$ is average reflection spectrum of all samples; a_i is linear translation coefficient; b_i is tilt migration coefficient; X_{i_msc} is the reflectance spectrum after multivariate scattering correction.

2.3.4 Sample set partitioning based on SPXY

Galvao proposed SPXY sample division method[18] on the base of Kennard-Stone (KS) method and Content Gradient method, taking both spectral space and property space of samples into account. According to the principle of SPXY, the *X* variables and

the *Y* variables are taken into account simultaneously. And in order to ensure that the distance has the same weight in the *X* and *Y* space respectively, $d_x(p,q)$ and $d_y(p,q)$ are divided by the maximum value in respective data set. The distance between the samples is calculated as Equation (9):

$$d_x(p,q)=\sqrt{\sum_{j=1}^{J}[x_p(j)-x_q(j)]^2};\ p,q\in[1,N] \quad (7)$$

$$d_y(p,q)=\sqrt{(y_p-y_q)^2};\ p,q\in[1,N] \quad (8)$$

$$d_{xy}(p,q)=\frac{d_x(p,q)}{\max_{p,q}\in[1,N]d_x(p,q)}+\frac{d_y(p,q)}{\max_{p,q}\in[1,N]d_y(p,q)} \quad (9)$$

2.3.5 IPLS

The sensitive spectral wavebands to chlorophyll content were selected by IPLS method. It is a wavebands selection method[19,20] based on partial least squares (PLS).

The basic principle of IPLS method is to divide the full waveband into N intervals uniformly. In each interval, the number of optimal factors is determined by the interactive verification method, and the corresponding PLS optimal model is established. Then, the RMSE corresponding to each PLS model is obtained. The spectral ranges whose RMSE are relative smaller will be selected, and all the wavebands in the selected spectral ranges will be used to establish prediction model. The RMSE indicator is calculated as Equation (10):

$$RMSE=\sqrt{\sum_{i=1}^{n}(y'-y)^2/n} \quad (10)$$

where, y' is predictive value and y is measured value; n is the number of samples.

2.3.6 SVR

The SVR method was proposed by Vapnik[21] on the basis of support vector machine (SVM). It was a modeling method specifically for small sample problems, which could be used to obtain optimal solutions with finite samples. SVR mapped original variables to high dimensional feature space by using the nonlinear transform, and then the linear classification function was conducted in high dimensional feature space, which ensured that the model had good generalization capacity and also solved the problem of "dimension disaster".

However, there is no specific theory at the selection of the parameters (i.e., the penalty parameter of *C* and the kernel function parameter of *g*) in SVR studying and training, which affect the prediction accuracy and efficiency of SVM modeling. Artificially parameters setting is always adopted on the basis of specific issues. According to the literatures, the better parameter combinations could be obtained after repeating designating each parameter and comparing their results, which might lead to inefficiency and blindness. Under normal conditions, *g* and a lower *C* are suggested since the model with the lowest predicting error could be established. The cross validation method helps to avoid over-fitting and to improve fitting efficiency[22].

This study adopted the cross validation method to realize the optimal parameters selection in SVR modeling. Firstly, the penalty parameter of *C* and the kernel function parameter of *g* were searched in a wide-range, the lowest training error was then observed. Then *C* and *g* could be searched in a specific narrow-range and more precise values could be determined. According to the experience, an exorbitant penalty parameter would lead a model with over-fitting, or high fitting coefficients but weak generalization.

The methods mentioned above were operated with the program in Matlab R2014a environment. In which wavelet denoising was realized by wavelet toolbox, and SVR was implemented by LIBSVM[23] software package.

3 Results and discussion

3.1 Characteristic analysis of field spectral

Because of the influence of the field environment and the instability of the instrument, there is always a lot of noise in the spectral data measured in field environment. To make sure whether there was significant noise in the signal collected in the field, the standard reflectance spectral of maize leaf was measured in lab. The mean values of two kinds of curves are shown in Figure 2. In general, the standard curve was smooth without significant fluctuation. Compared with the standard spectral, there was obvious fluctuation noise signal of the field canopy reflectance in the range of 325-400 nm and 900-1075 nm. Except the two ranges discussed above, some of the noise phenomena were showed in others wavelengths (400-900 nm). So it was necessary to denoise the spectral data measured in field environment.

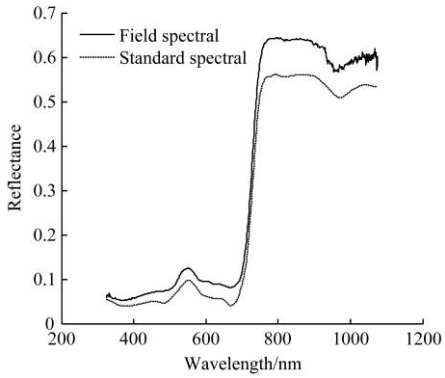

Figure 2 Comparison of field and standard spectral

3.2 Wavelet denoising

To eliminate the noise influence, the wavelet denoising algorithm was used. The paper employed SNR and CS to evaluate the wavelet denoising effect and to help determine the suitable wavelet basis function and decomposition level.

In general, the wavelet basis function and decomposition level are the most two important factors in the wavelet denoising, although the SymN (N=2, 3, …, 8) wavelets were shown as the alternative wavelet functions because of its orthogonal symmetry property and compactly supported property. The best performing wavelet function and decomposition level should be determined. There were two steps as follows:

Firstly, the decomposition level was fixed to 5 according to some relevant researches[24-26] in order to select the best performing wavelet**.** Thus, the parameter settings of wden() function were the 5 decomposition level, 'hursure' threshold selection, soft thresholding and "sln" threshold rescaling. When different symN wavelet basis functions were used, the evaluation indicator values were calculated. The denoised spectral reflectance under different symN wavelet is shown in Figure 3. The indicator values are shown in Table 1.

Overall, the change trends of SNR and CS were reversed. The values of SNR increased firstly and then decreased, while the CS values increased after decreased. Specifically, SNR values increased from 101.65 (Sym2) to 106.67 (Sym6) and decreased to 103.15 (Sym7), then rose to 104.41 (Sym8). The largest value of SNR was 106.67 on Sym6 wavelet operation. Meanwhile, the CS

values decreased from 75.14 (Sym2) to 41.28 (Sym7) and then rose to 42.54 (Sym8). The values of CS were nearly after the Sym6. Comprehensive considering the SNR and CS, the Sym6 wavelet was selected as the basis function.

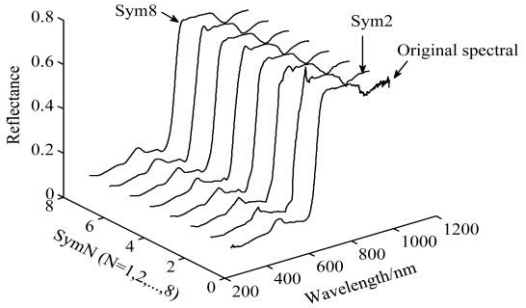

Figure 3 Denoised spectral curve under different SymN

Table 1 Evaluation indicator values of SymN wavelets

wavelet	*SNR*	*CS*
Sym2	101.65	75.14
Sym3	103.17	49.07
Sym4	104.58	44.63
Sym5	104.85	43.05
Sym6	106.67	42.82
Sym7	103.15	41.28
Sym8	104.41	42.54

Secondly, the 'wname' parameter of the wden() function was fixed to be the Sym6 wavelet to evaluate the denoising effect of different decomposition levels by SNR and CS. The other parameters of the wden() function were kept the same. When different decomposition layers were used, the evaluation indicator values were calculated. The denoised spectral curves of a sample after 1st-8th layer decomposition by Sym6 wavelet are shown in Figure 4. The corresponding indicator values are shown in Table 2.

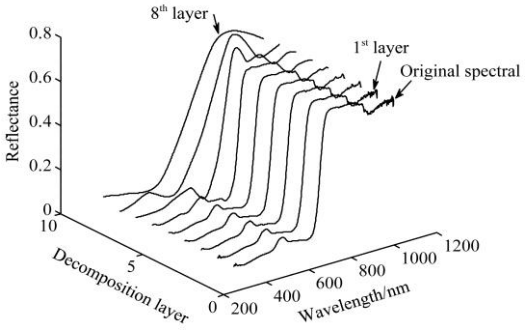

Figure 4 1st-8th layer wavelet decomposition curves of the spectral data

Table 2 Evaluation indicator values of 1st-8th decomposition layer

layers	*SNR*	*CS*
1	136.24	65.96
2	123.98	46.73
3	119.81	43.76
4	113.76	43.01
5	106.67	42.82
6	89.85	31.21
7	78.12	15.91
8	78.74	11.43

According to Figure 4, with the increasing decomposition scale, the obtained curves became smoother because of the eliminating of random noise. And after 5th layer, some deformation obviously appeared in the denoised spectral curve because of the loss of useful information.

As shown in Table 2, from 1st layer to 5th layer, both the SNR and CS values slowly decreased with the increasing decomposition scale, in which the SNR was decreased from 136.24 to 106.67 and CS was decreased from 65.96 to 42.82. And then from 5th layer to 8th layer, they decreased remarkably with SNR from 106.67 to 78.74 and CS from 42.82 to 11.43. It was shown that the SNR values were similar between the 7th layer and 8th layer with 78.12 and 78.74 respectively.

According to the definition of SNR, when the denoising effect is very small, the indicator value would still be large enough to meet the requirements, but it did not actually achieve the purpose of denoising. So CS was used as an auxiliary indicator to evaluate the denoising effect. Although the SNR value of 1st layer was the largest (136.24), there was still obviously fluctuation as the CS value was 65.96. In the 5th layer, the SNR was 106.67 and the CS value was 42.82. Their properties are much better than that of the 1st layer and without signal distortion. The result indicated that the 5th layer decomposition could remove most of the noise without losing useful noise. Thus, the 5th layer decomposition was determined with the best denoising effect based on the SNR and CS evaluation comprehensively.

As a result, the Sym6 wavelet under 5th layer decomposition was used to denoise the original spectral data. The original spectral data is shown in Figure 5a and the denoised spectral data is shown in Figure 5b. The denoised spectral curves were much smoother than the original spectral curve, especially in the range of 325-400 nm and 900-1075 nm. In addition, the slight fluctuations were also filtered within 400-900 nm. It was indicated that most of the noise had been removed and the quality of the field spectral reflectance data was improved.

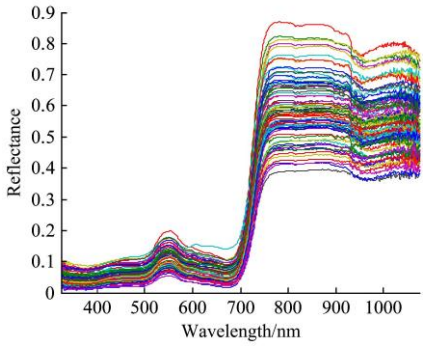

a. Original Spectral

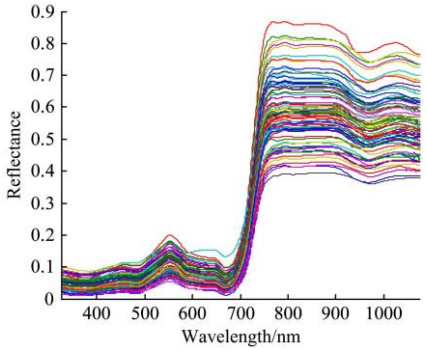

b. Denoised Spectral

Figure 5 Result of spectral denoising

3.3 MSC

The problems of baseline shift and offset always exist in the canopy diffuse emission because of the scatter interference from the crossover and overlaps of maize leaves. Therefore, as shown in Figure 5, there were obviously overlaps in the range of 325-750 nm and the spectral reflectance varied considerably in the near infrared range of 750-1075 nm. In order to reduce the influence of baseline shift and offset caused by scattering, the denoised spectral reflectance was processed by MSC. The corrected spectral curves are shown in Figure 6. The results showed that the baseline shift and offset of each spectral curve were corrected.

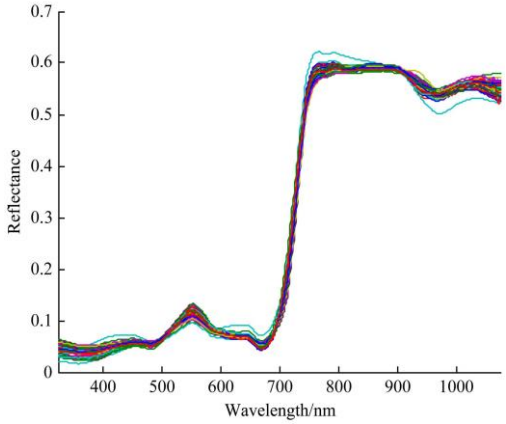

Figure 6 Spectral after MSC

3.4 Sensitive wavebands determination

After the data sets division by SPXY, 60 samples were used as modeling set and 20 samples were used as verification set. The statistical results of chlorophyll content in each data set are shown in Table 3.

Table 3 Statistical results of divided data set

	Num	Max	Min	Mean	Std
All data	80	51.66	35.66	42.93	3.16
Modeling	60	51.66	35.66	42.96	3.23
Verification	20	48.87	37.30	42.85	3.03

The operation of selecting sensitive wavebands was conducted on the modeling set. The spectral reflectance of samples in modeling set from 325 nm to 1075 nm was analyzed by using IPLS with the window width of 25. A total of 30 windows were obtained. A PLS model for predicting chlorophyll content was established by using all the wavebands in each window. The performance of each model was evaluated by RMSE. The RMSE for this series of 30 models were shown in Figure 7. The statistical results of RMSE for each window are shown in Table 4.

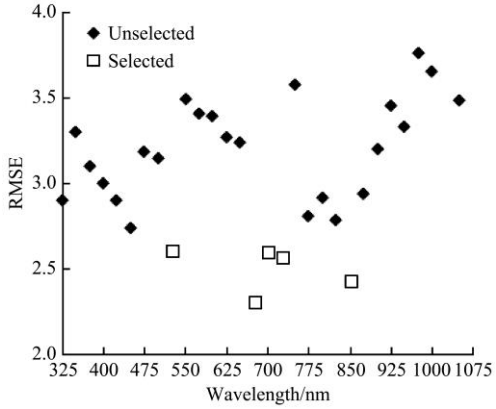

Figure 7 Selected Wavelengths by IPLS

Table 4 Statistical result of RMSE for each window

Max	Min	Mean	Std
3.78	2.31	3.09	0.38

The five spectral ranges whose RMSE (2.31, 2.44, 2.57, 2.60, 2.61 respectively) were smaller than others (shown as "□" in Figure 7). After consecutive ranges merged, the finally obtained spectral ranges were: 525-549 nm, 675-749 nm and 850-874 nm.

According to the spectral response characteristics of green plants[27], the range of 525-549 nm was in the strong reflectance region of chlorophyll. The range of 675-749 nm was red-edge range influenced by absorption of chlorophyll, which is easily moved by the changes of near infrared reflectance. Although the absorption of chlorophyll in near infrared band was not as much as in visible band, the 850-874 nm range is in the region of high reflectance platform which is the significant characteristic of vegetation. It was indicated that the selected bands could be used to estimate the chlorophyll content.

3.5 Chlorophyll content prediction modeling by SVR

Although the selected bands presented the spectral properties of vegetation, there might be some nonlinear relationship between chlorophyll content and the selected sensitive wavebands especially in 850-874 nm. SVR modeling method is based on the minimization principle of structural risk, which shows many advantages in solving pattern recognition such problems as small sample set, non-linear, high dimensional pattern and local minimum values. Thus, it was determined to be used to establish the chlorophyll content prediction model.

A SVR prediction model of chlorophyll content was established by using all the sensitive wavebands in the ranges of 525-549 nm, 675-749 nm and 850-874 nm selected by IPLS. The SVR model is shown in Figure 8. The calibration R_c^2 of the model reached to 0.831 and the RMSEC was 1.3852 mg/L; the validation R_v^2 reached to 0.809, the RMSEP was 0.8664 mg/L.

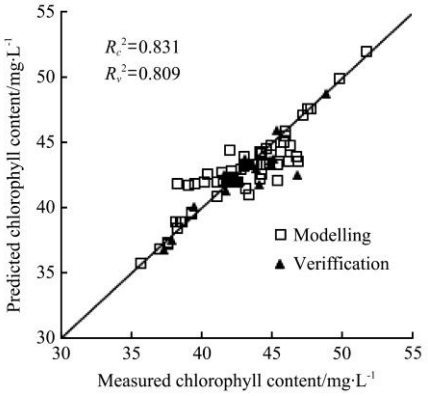

Figure 8 SVR Model for predicting chlorophyll content

4 Conclusions

This research aimed to rapidly and non-destructively estimate the chlorophyll content of maize using spectroscope. Firstly, the spectral reflectance and chlorophyll content of canopy were measured. Then, the spectral signals were denoised and corrected, and the sensitive spectral ranges were selected. Finally, a SVR model for predicting estimating chlorophyll content was established. The main conclusions are as follows:

(1) Sym6 wavelet function and the 5th level wavelet decomposition were chosen for denoising the original spectral data based on *SNR* and *CS* evaluation. The baseline translation and offset were eliminated by MSC method.

(2) The three spectral ranges including 525-549 nm, 675-749 nm and 850-874 nm were selected for chlorophyll content predicting by IPLS based on the RMSE evaluation.

(3) A SVR model for predicting chlorophyll content was established. The calibration R_c^2 of the SVR model reached to 0.831, the RMSEC was 1.3852 mg/L, and the validation R_v^2 reached to 0.809, the RMSEP was 0.8664 mg/L. The results indicated that the SVR model could be used to estimation the chlorophyll content of maize canopy in the field.

Acknowledgements

This study was supported by the Chinese High Technology Research and Development Research Fund (2016YFD0300600 -2016YFD0300606, 2016YFD0300600-2016YFD0300610), NSFC program (31501219), the Fundamental Research Funds for the Central Universities (2018TC020, 2018XD003), and Industry Research Project (QingPu 2017-12).

[References]

[1] Xie C Q, Yang C, A H J, Gregg A J, Forrest T I. Spectral reflectance response to nitrogen fertilization in field grown corn. International Journal of Agricultural and Biological Engineering, 2018; 11(4): 118–126.

[2] Ramoelo A, Dzikiti S, van Deventer H, Maherry A, Cho M A, Gush M. Potential to monitor plant stress using remote sensing tools. Journal of Arid Environments, 2015; 113(2): 134–144.

[3] Kalacska M, Lalonde M, Moore T R. Estimation of foliar chlorophyll and nitrogen content in an ombrotrophic bog from hyperspectral data: Scaling from leaf to image. Remote Sensing of Environment, 2015; 169: 270–279.

[4] Huang W J, Lu J J, Ye H C, Kong W P, Mortimer A H, Shi Y. Quantitative identification of crop disease and nitrogen-water stress in winter wheat using continuous wavelet analysis. International Journal of Agricultural and Biological Engineering, 2018; 11(2): 145–152.

[5] Ciganda V, Gitelson A, Schepers J. Non-destructive determination of maize leaf and canopy chlorophyll content. Journal of Plant Physiology, 2009; 166(2): 157–167.

[6] Chen P F, Haboudance D, Tremblay N, Wang J H, Vigneault P, Li B G. New spectral indicator assessing the efficiency of crop nitrogen treatment in corn and wheat. Remote Sensing of Environment, 2010; 114(9): 1987–1997.

[7] Schlemmer M, Gitelson A, Schepers J, Ferguson R, Peng Y, Shanahan J, et al. Remote estimation of nitrogen and chlorophyll contents in maize at leaf and canopy levels. International Journal of Applied Earth Observation and Geoinformation, 2013; 25: 47–54.

[8] Rossini M, Cogliati S, Meroni M, Migliavacca M, Galvagno M, Busetto L, et al. Remote sensing-based estimation of gross primary production in a subalpine grassland. Biogeosciences, 2012; 9(7): 2565–2584.

[9] Sun H, Zhao Y, Zhang M, Wen Y, Li M Z, Yang W, et al. Multi-spectral image detection for maize canopy's chlorophyll content in jointing stage. Transactions of the CSAE, 2015; 31(Supp.2): 186–192. (in Chinese)

[10] Deng X L, Li M Z, Zheng L H, Zhang Y, Sun H. Estimating chlorophyll content of apple leaves based on preprocessing of reflectance spectra. Transactions of the CSAE, 2014; 30(14): 140–147.

[11] Chu X L, Yuan H F, Lu W Z. Progress and application of spectral data pretreatment and wavelength selection methods in NIR analytical technique. Progress in Chemistry, 2004; 16(4): 528–542. (in Chinese)

[12] Ding Y J, Li M Z, Zheng L H, Zhao R J, Li X H, An D K. Prediction of cholorphyll content of greenhouse tomato using wavelet transform combined with NIR spectra. Spectroscopy and Spectral Analysis, 2011; 31(11): 2936–2939. (in Chinese)

[13] Daubechies I. The wavelet transform, time-frequency localization and signal analysis. IEEE Transactions on Information Theory, 1990; 36(5): 961–1005.

[14] Li T H, Shi G Y, Wei M, Wang J M, Hou J L. Wavelet denoising in prediction model of tomato Vitamin C content using NIR spectroscopy. Transactions of the CSAM, 2013; 44(S1): 200–204. (in Chinese)

[15] Liang L, Yang M M, Zang Z. Determination of wheat canopy nitrogen content ratio by hyperspectral technology based on wavelet denoising and support vector regression. Transactions of the CSAE, 2010; 26(12): 248–253. (in Chinese)

[16] Martens H, Stark E. Extended multiplicative signal correction and spectral interference subtraction: New preprocessing methods for near infrared spectroscopy. Journal of Pharmaceutical & Biomedical Analysis, 1991; 9(8): 625–635.

[17] Maleki M R, Mouazen A M, Ramon H, De Baerdemaeker J. Multiplicative scatter correction during on-line measurement with near infrared spectroscopy. Biosystems Engineering, 2007; 96(3): 427–433.

[18] Galvão R K H, Araujo M C U, José G E, Pontes M J C, Silva E C, Saldanha T C B. A method for calibration and validation subset partitioning. Talanta, 2005; 96(4): 736–740.

[19] Zhou X H, Xiang B R, Wang Z M, Zhang M. Determination of quercetin in extracts of ginkgo biloba l. leaves by near - infrared reflectance spectroscopy based on interval partial least squares (iPLS) model. Analytical Letters, 2007; 40(18): 3383–3391.

[20] Nørgaard L, Saudland A, Wagner J, Nielsen J P, Munck L, Engelsen S B. Interval partial least-squares regression (iPLS): A comparative chemometric study with an example from near-infrared spectroscopy. Applied Spectroscopy, 2000; 54(3): 413–419.

[21] Vapnik V N. The nature of statistical learning theory. New York: Springer-Verlag, 1995.

[22] Igne B, Reeves J I, Mccarty G, Hively W, Lund E, Hurburgh C. Evaluation of spectral pretreatments, partial least squares, least squares support vector machines and locally weighted regression for quantitative spectroscopic analysis of soils. J. Near Infrared Spectrosc, 2010; 18(3): 167.

[23] Chang C C, Lin C-J. LIBSVM: A library for support vector machines. 2001.

[24] Cen H Y, He Y, Zhang H, Feng F Q. Rapid measurement of citric acids in orange juice using visible and near infrared reflectance spectroscopy. Spectroscopy and Spectral Analysis, 2007; 27(9):1747–1750.

[25] Wang G Q, Wang W, Fang Q Q, Jiang H, Xin Q C, Xue B L. The application of discrete wavelet transform with improved partial least-squares method for the estimation of soil properties with visible and near-infrared Spectral Data. Remote Sens, 2018; 10(6): 867–884.

[26] Yi T, Li H, Zhao X. Noise smoothing for structural vibration test signals using an improved wavelet thresholding technique. Sensors, 2012; 12(8): 11205–11220.

[27] Li M Z. Spectral analysis technique and its application. Beijing: Science Press, 2006; pp.176–180.